REPORT DOCUMENTATION PAGE

Form Approved
OMB No. 0704-0188

1. AGENCY USE ONLY (Leave blank)
2. REPORT DATE: 1995
3. REPORT TYPE AND DATES COVERED: Interim

4. TITLE AND SUBTITLE
Electronic Structure of Donor-spacer-Acceptor Molecules of Potential Interest for Molecular Electronics III: Geometry and Absorption Spectrum of CH_3-αP3CNQ

5. FUNDING NUMBERS
N00014-90-J-1608
G

6. AUTHOR(S)
Anders Broo and Michael C. Zerner

7. PERFORMING ORGANIZATION NAME(S) AND ADDRESS(ES)
University of Florida
Department of Chemistry
Gainesville, FL 32611 USA

8. PERFORMING ORGANIZATION REPORT NUMBER

9. SPONSORING/MONITORING AGENCY NAME(S) AND ADDRESS(ES)
Office of Naval Research
Chemistry Division Code 1113
Arlington, VA 22217-5000

10. SPONSORING/MONITORING AGENCY REPORT NUMBER
Technical Report 26

11. SUPPLEMENTARY NOTES
Molecular Physics, In Press

12a. DISTRIBUTION/AVAILABILITY STATEMENT
This document has been approved for public release: its distribution is unlimited.

12b. DISTRIBUTION CODE

13. ABSTRACT (Maximum 200 words)

See attached Abstract.

14. SUBJECT TERMS

15. NUMBER OF PAGES
28

16. PRICE CODE

17. SECURITY CLASSIFICATION OF REPORT	18. SECURITY CLASSIFICATION OF THIS PAGE	19. SECURITY CLASSIFICATION OF ABSTRACT	20. LIMITATION OF ABSTRACT
Unclassified	Unclassified	Unclassified	SAR

OFFICE OF NAVAL RESEARCH

GRANT or CONTRACT N00014-90-J-1608

R&T CODE 4131057- - - 01

Technical Report No. 26

Electronic Structure of Donor-spacer-Acceptor Molecules of Potential Interest for Molecular Electronics III: Geometry and Absorption Spectrum of CH_3-αP3CNQ

by

Anders Broo and Michael C. Zerner

Prepared for Publication or Published

in

Molecular Physics

University of Florida
Department of Chemistry
Quantum Theory Project
Gainesville, FL 32611-8435

April 18, 1995

Electronic Structure of Donor-spacer-Acceptor Molecules of Potential Interest for Molecular Electronics III: Geometry and Absorption Spectrum of CH3-αP3CNQ.

by

Anders Broo[a] and Michael C. Zerner
Quantum Theory Project
University of Florida
Gainesville, Florida 32611-8435

Abstract:

The geometry of Z-β-(1-methyl-2-pyridinium)-α-cyano-4-styryldicyanomethanide was optimized using semi-empirical and *ab initio* quantum chemical methods. The predicted geometries using a one determinant description do not compare well with the observed geometry. A better description of the geometry is obtained with a multi-determinant approach. Good agreement with experiment is obtained only when cosideration of the media is taken into account. Absorption spectra in the solid state and in solution were calculated and the results compare very well with the experimental spectra. The solvatochromic shift of the absorption spectrum was calculated using a self-consistent reaction field approach. We also discuss the question of whether the title molecule is best described as a zwitterion.

---

a) Permanent address Department of Physical Chemistry, Chalmers University of Technology, 412 96 Göteborg, Sweden.

1. Introduction.

In a previous series of papers the electronic structure of organic molecules of the type electron Donor-bridge-Acceptor (D-b-A), that are of potential interest for molecular electronics, have been investigated [1]. The aim of these studies is, primarily, to get more knowledge about the properties of these molecules and how they relate to the electronic structure, and, secondly, to determine the limitations of the calculational methods that we are using for these studies. Since, in general, the molecules of interest are large molecules, the use of correlated *ab initio* calculations is all but impossible, and recourse must be taken to semi-empirical methods. When using these approximate methods, it is important to get an idea of how large the eventual errors may be. Therefore comparisons with experiment and with the best affordable *ab initio* calculations are most useful.

In this work and in a following paper [2] molecules of the D-b-A type with a strong electron donor and a good electron acceptor are investigated by means of quantum mechanical calculations at several different levels of sophistication. Systems of potential interest have been investigated by Ashwell [3], in which he studied the optical properties of Z-β-(1-hexadecyl-4-pyridinium)-γ-cyano-4-styryldicyanomethanide ($C_{16}H_{33}$-P3CNQ) and Z-β-(1-hexadecyl-4-quinolinium)-γ-cyano-4-styryldicyanomethanide ($C_{16}H_{33}$-Q3CNQ) and their α-bridged analogues, see figure 1 [3]. The absorption spectra of both $C_{16}H_{33}$-P3CNQ and $C_{16}H_{33}$-Q3CNQ show very interesting features. If a Langmuir-Blodgett (L-B) film of these molecules (blue-green color) is irradiated with light corresponding to the wave length of the charge transfer band in the absorption spectra, the color of the film disappears. In solution the bleaching effect vanishes after some minutes but in the L-B film the effect is permanent. The geometry and absorption spectra of P3CNQ and Q3CNQ will be investigated in a forthcoming paper [2]. In this work we concentrate on Z-β-(1-methyl-2-pyridinium)-α-cyano-4-styryldicyanomethanide (α-P3CNQ), one of the molecules that Ashwell has studied in great detail.

* Figure 1 *

The crystallographic geometry and a preliminary absorption spectrum of α-P3CNQ were presented some years ago by Metzger, Heines and Ashwell [4]. They concluded that the ground state of α-P3CNQ was of zwitterionic type due to the large dipole moment and the observation that the central bond in the bridge was close to that expected for a typical carbon-carbon double bond. The dipole moment was calculated to be 26.16 Debye, using the crystal geometry in a closed shell INDO calculation [4]. Somewhat later, Akhtar, Tanaka, Metzger and Ashwell reported the spectra of α-

P3CNQ in solid state and in solution [5]. In this work we obtain the geometry of α-P3CNQ using different theoretical approaches, and compare the results with the crystallographic geometry. In order to address the zwitterionic nature of the ground state of α-P3CNQ we will see that classification into extreme types as either zwitterionic or "neutral" is not possible.

We begin this study by investigating the electron structure and geometry of α-P3CNQ and determine how sensitive these results are to computational method and to basis set. We then investigate the effects that solvation have in determining the ground state properties and absorption spectra.

2. Methods.

2.1 Geometry optimization.

The geometry optimization was performed at several levels of theory. The ground state geometry, assuming a closed-shell electronic configuration, was calculated using the semi-empirical AM1 and PM3 methods [6]. The closed-shell ground state geometry was also optimized with *ab initio* methods with three different basis sets, one with the minimal basis set STO-3G (HF/STO-3G) [7a], one with a split-valence double-zeta basis set 3-21G [7b] (HF/3-21G) and one split-valence double-zeta valence basis plus a polarization function for the "heavy" atoms (HF/6-31G*) [8]. The AM1 and PM3 calculations were performed with both the MOPAC 6.01 program package [6] and with the GAMESS program package [9]. The *ab initio* calculations were performed with the GAMESS program. Since α-P3CNQ is a large molecule, the practical use of *ab initio* methods dictates the use of moderate sized basis sets. Even so, with the relative small basis set (3-21G) it was not possible to store the integrals on disk. Hence, the geometry optimization with the large basis sets was carried out using direct SCF. With the STO-3G basis set a total of 122 contracted basis functions was used; with the 3-21G basis set 222 contracted basis functions were used; the 6-31G* basis generates 354 contracted basis functions.

α-P3CNQ has 96 degrees of internal freedom. Even using a semi-empirical theory, as for example the AM1 model, a geometry optimization is rather time consuming and care must be taken to select the best set of coordinates to be used in the geometry optimization. We found, from many computer experiments, that using Cartesian coordinates and a convergence threshold $g_{max} < 0.0005$ Hartree/Bohr gives a good compromise between CPU time and accuracy.

A minimum requirement to describe a biradical or a zwitterion is to include determinants where electrons have been excited from the highest occupied molecular orbital (HOMO) to the lowest unoccupied molecular orbital (LUMO). This can be achieved by a multi-configuration SCF treatment or by a generalized valence bond (GVB) calculation with one geminal pair, sometime called two-configuration SCF (TCSCF). By performing either of these calculations we account for some of the very important electron correlation that is necessary to describe this type of charge separated state. In a semi-empirical calculation most of the dynamic electron correlation is assumed to be included *via* the parametrization. However, to be able to treat biradical states and charge separated states we have to include the non-dynamic correlation, not accounted for by the parametrization, in the calculation. This is done by the "half electron method" [6d] followed by a small configuration interaction (CI) calculation [6 e,f]. The CI space is restricted to excitations from HOMO to LUMO resulting in 4 configurations (three singlet states and one triplet state). Thus, we performed geometry optimizations of α-P3CNQ using this 4x4CI method. All efforts to optimize this biradical state using an *ab initio* GVB method with one geminal pair failed with the two larger basis sets. The only *ab initio* GVB calculation that converged was with the minimal basis and the geometry obtained from this optimization was exactly the same as that obtained with the RHF/STO-3G calculation. Open-shell singlet (two electrons in two open-shells) geometry optimization has the same problem with convergence in the SCF step as does the GVB calculations. The only *ab initio* open-shell calculation that did not have convergence problem was the restricted open-shell Hartree-Fock (ROHF) calculation for the triplet state. A ROHF triplet state geometry optimization with the STO-3G basis was also done even though experimentally α-P3CNQ is known to have a singlet ground state [4].

To investigate the importance of electron correlation a geometry optimization at the second-order Møller-Pleset perturbation theory with the STO-3G basis set (MP2/STO-3G) level was performed. The usage of MP2 calculations with minimal basis is, of course, of limited value, but we are interested in estimating how important the correlation correction might be in obtaining the geometry in this type of system. The MP2 calculation was performed with the Gaussian92 program [10].

2.2 Absorption spectra.

All absorption spectra were calculated with the INDO/S Hamiltonian using the ZINDO program package [11]. The solvent influence on the calculated spectra is accounted for via the self-consistent reaction field (SCRF) method [12]. The absorption spectra were calculated from CI calculations that includes single excitations only, CIS. The active space in the CI calculations include all $\pi \rightarrow \pi^*$ transitions and all cyano $n \rightarrow \pi^*$ transitions.

3. Results and discussion.

3.1 Geometry optimization of α-P3CNQ

It is possible to draw at least one neutral and three zwitterionic resonance structures of α-P3CNQ, see figure 2.

* fig. 2 *

If we consider the "neutral" resonance structure, figure 2a, we find an alternation of the carbon-carbon bond lengths between single and double bonds. Furthermore, the bridge bond (C1-C2) is a single bond. This resonance structure is the structure that we expect to find when we optimize the geometry with a RHF calculation, since a single determinant description favors an uncharged structure. In the zwitterionic resonance structures the acceptor has delocalized electrons and near equal C-C bonds. The donor part of the molecule has a positive charge localized either on C16, C18 or C21. The C-C bonds lengths alternate. Furthermore, the bridge C-C bond is a double bond. The bridge geometry found in experiment clearly suggest a zwitterionic resonance structure, while the donor and the acceptor geometries suggest a mixture of all three resonance structures' 2b-d.

The optimized ground-state geometries of α-P3CNQ obtained from restricted Hartree-Fock (RHF) calculations are compared with the crystallographic geometry in Table 1. Both semi-empirical and *ab initio* RHF optimizations yield similar geometries. The main differences between the experimental geometry and those calculated are found in the bridge. The torsion angle between donor and bridge (α) is calculated to be smaller than observed. The torsion angel between bridge and acceptor unit (β) is calculated to be somewhat larger than observed. Finally, the torsion angle around the ethylene "double" bond (γ) is much larger in all calculations than observed experimentally. The angle γ is calculated much larger than the experimental torsion angle because the central bond in the cyano-ethylene group is calculated to be much longer than a formal C-C double bond. The RHF type calculations suggest a resonance mix of the structures showed in Figure 2a, 2b and 2d, neither zwitterionic nor "neutral".

Since the geometries obtained at the RHF level did not agree very well with experiment an additional set of calculations was performed. First a 4x4CI/AM1 and a 4x4CI/PM3 geometry optimization were performed. By mixing configurations in this fashion we increase the flexibility of the wave function, which does not necessarily lead to a different state, but rather a better description of

the state. The optimized geometries using this procedure are summarized in Table 2. Comparing the semi-empirical 4x4 CI geometries with the RHF geometries we find the geometry of the donor group almost unchanged. The bond alternation obtained for the acceptor is now much reduced. The largest differences between the two calculations are again observed in the bridge.

As mentioned in the previous section, all *ab initio* geometry optimizations of a singlet zwitterion state failed except the GVB/STO-3G optimization which gave the same geometry as the HF/STO-3G optimization. However, a ROHF/STO-3G geometry optimization for the triplet state was also performed. A summary of the geometry obtained in the triplet calculation is found in table 2. The triplet state geometry agrees very well with the observed geometry, although the ground state is known experimentally to be a singlet [4]. The triplet state is predicted to be higher in energy by 385 cm^{-1} than the lowest singlet state at the HF/STO-3G level. (This value might be considered the lower limit as HF calculations generally artificially favor triplet state over closed-shell singlet state by about 10000 cm^{-1} [13]. The predicted singlet triplet energy difference then would be about 10500 cm^{-1})

To estimate how important electron correlation is for the geometry of α-P3CNQ a MP2 geometry optimization was performed. The MP2 calculation must be considered as preliminary since the basis set we are restricted to use is far too small to account very well for electron correlation. However, what we can achieve with this calculation is a trend when correcting for electron correlation. The geometry obtained at the MP2/STO-3G level differs rather much from the geometry at the HF/STO-3G level. The MP2/STO-3G geometry is almost planar and all three torsion bridge angles are close to 0 degrees. The C1-C2 bond is a little shorter and the C2-C3 and C1-C16 bonds are much longer resulting in a more or less delocalized pictured, that does not agree well with the experimental geometry, see Tables 1 and 2.

The best agreement between the observed crystallographic geometry and the calculated geometry is obtained in the 4x4CI/PM3 calculation. Since α-P3CNQ is a rather polarizable molecule one might assume that the electrostatic effects on the geometry might be significant. As we will see in the next section the dimer interaction is very large in the crystal. We did one geometry optimization of the dimer using the HF/AM1 approach. This calculation did not alter the picture that we have just reported. The dimer unit might be too small to account for all the electrostatic effects that might help to stabilize the zwitterionic form of α-P3CNQ. Another way to account for electrostatic effects is to optimize the geometry in a reaction field, which describes the surrounding matter as a continuum. We did two geometry optimizations with the SCRF/AM1 method with two different cavity radii a_0 and an ε equal to that of acetonitrile, see Table 2. With the smallest a_0, corresponding to the largest dimension

of the molecule, we obtain a very good agreement between the predicted geometry and the observed one. This supports the idea that the zwitterionic form is stabilized by electrostatic effects both in solution and in the solid state. With the somewhat larger cavity size we predict a geometry that is close to what is predicted in the 4x4CI/PM3 and 4x4CI/AM1 calculations.

In table 3 the Mulliken atomic charges and dipole moment are summarized. All atomic charges and dipole moment are calculated using the optimized geometries. It is clear from the table that the atomic charges vary with basis set and between semi-empirical and *ab initio* calculations. What is important here are relative charges within a given basis set or model. If we sum up the charges for the donor, bridge and acceptor, respectively, we find that the group charges compare reasonably well among the different types of approaches used. The calculated Mulliken charges show that C16 is positively charged, partly showing a bias for structure 2b. All the RHF calculated geometries resemble the zwitterionic resonance structure of the donor and the Mulliken charge of C16 is large and positive. The bridge and the acceptor clearly resembles the neutral resonance structure. The 4x4CI/AM1 and 4x4CI/PM3 geometries also suggests the same mixture of resonance structures as was found for the RHF calculated geometries. However, the bridge bond lengths are calculated as equal and correspond to delocalization. Clearly all three resonance structures are important and have almost the same energy. Furthermore, the electronic distribution is not very sensitive to the change in geometry. This is likely the reason why the convergence rate of the geometry optimization is so slow. It is difficult to tell which simple picture, neutral or zwitterionic, is the "true" one. The best agreement between crystallographic geometry and the calculated geometry, not including the reaction field predicted geometry, is obtained using the PM3 Hamiltonian and the 4x4 CI approach, which yields a wave function which is almost 72 % closed-shell 16% open-shell (biradical) and 12 % double excited configuration that add zwitterionic character to the single determinant description. The 4x4CI/AM1 calculation is as good for bond lengths, but slightly worse for the rotation angle.

The proofs for a zwitterionic structure, put forward by Ashwell et al. [5], included (1) the double bond character of the bridge bond (C1-C2), (2) the calculated dipole moment using a RHF/INDO calculation with the experimental geometry (26.16 Debye) and (3) the position of the C-N stretching band of the IR-spectrum, which is very sensitive to the charge distribution [3]. Their first point was discussed above, and is, in fact, strong evidence. Their second point is doubtful since we found that a single determinant description is not sufficient to describe the ground state. Using the four determinant description in a AM1 calculation, the dipole moment has decreased dramatically to 9.52 Debye compared to the RHF/AM1 dipole moment of 21.51 Debye. Their third point is harder to investigate by means of quantum chemical calculations since we need to include correlation effects to describe the

vibrational spectrum with the accuracy required here. However, HF calculated frequencies usually scale approximate linearly with scale factors ranging from 0.85 to 0.90. The vibration spectrum calculated by RHF/AM1 and scaled by a factor of 0.85 is depicted in figure 3. The band shape of the calculated IR-spectrum is obtained by using Gaussian functions centered at each calculated peak. The band width was set arbitrarily to 5 cm^{-1}.

* fig. 3 *

In the experimental IR-spectrum of α-P3CNQ the nitrile stretching double peak is located at 2175 cm^{-1} and 2135 cm^{-1}. In the calculated IR-spectrum we find a (scaled) triplet of states at 2173 cm^{-1}, 2161 cm^{-1} and 2160 cm^{-1}. The low intensity of these peaks is probably due to the small atomic charges of the atoms in the nitrile groups and a small induced dipole moment associated with these vibrations. Furthermore, the intensities are not often well described at the HF level of theory. Several peaks appear in the calculated spectrum at about 2700 cm^{-1} that corresponds to C-H stretching vibrations. Between 1000 cm^{-1} and 1500 cm^{-1} we find many intense peaks, the peaks around 1000 cm^{-1} are due to in-plane bending of the C-H bonds as well as the C-C bonds while the peaks around 1500 cm^{-1} are due to deformations of the phenyl ring systems and C-C bond stretching. The calculated IR-spectrum compares reasonably well with the IR-spectrum of $C_{16}H_{33}$-Q3CNQ [14]. The calculated IR-spectrum is by no way any proof for the neutral resonance structure since we do not know how sensitive the calculated spectrum is to the electronic structure. However, since all frequencies calculated are real we know that we have reached a minimum of the potential energy surfaces. Other structures were probed and either lead to the structure presented here or structures of considerable higher energies. Inspecting the low energy vibrational modes, at around 100 cm^{-1}, we find several modes that can transform the bridge to a zwitterionic form; however, these modes are, in general, quite complicated.

3.2 Absorption spectrum of α-P3CNQ.

3.2.1 Solid state absorption spectra.

The experimental absorption spectrum of the crystal (100) face shows a weak peak at 12400 cm^{-1} (parallel to the crystallographic b-axis) and 11800 cm^{-1} (perpendicular to the crystallographic b-axis) [5]. In the perpendicular spectrum a sharp intense peak appears at 21800 cm^{-1}. At higher energies unresolved bands are found for both polarizations. The spectrum observed on the (001) face showed a

weak peak at 12400 cm^{-1} (parallel) and the perpendicular spectrum has a very intense and broad band at 18600 cm^{-1} and a shoulder like band at 32000 cm^{-1}. The three low energy peaks were assigned to intermolecular charge transfer (INCT) band and the two bands at 18600 cm^{-1} and 21800 cm^{-1} were assigned to be intramolecular charge transfer (IRCT) bands. In table 4 the INDO/S calculated absorption spectra are compared with the experimental spectrum. In the INDO/S calculations we have used the crystallographic geometry for both the monomer and the dimer. In the calculated spectrum of the monomer the first band is found at 14138 cm^{-1} with a large oscillator strength. This band is due to a HOMO to LUMO transition and has charge transfer character (IRCT). The next peak is calculated at 19469 cm^{-1} and has a much smaller oscillator strength. This transition is due to a HOMO to LUMO+1 transition and also has charge transfer character, IRCT. In the dimer the MO's are grouped in pairs and the interaction between the two units is large. Each of the frontier MO's are delocalized over the whole dimer. Thus, each peak of the spectrum now contains two excitations. The first band has a dimer splitting of 1690 cm^{-1} and the major intense peak is found at 15096 cm^{-1}. Since the MO's are delocalized over the dimer and each peak is due to two configurations the net effect is that the character of this transition is no longer a charge transfer transition but more of a local transition. The dipole moment of both the ground state and most of the excited states are close to zero. Thus, we interpret the first peak of the experimental spectrum as due to the dimer split band. The dimer splitting is 6200 cm^{-1} and the major intense peak is the peak at 18600 cm^{-1}. With this interpretation there is no intermolecular charge transfer absorption. The second allowed transition in the calculation is found at 21232 cm^{-1} and compares very well with the experimental band at 21800 cm^{-1}. Our conclusion is that the dimer interaction is very strong and this interaction helps to stabilize the zwitterionic conformation in the crystal.

3.2.2 Solution absorption spectra.

First we investigate the self-consistent reaction field (SCRF) model dependence. In this test the crystallographic geometry was used to be consistent. The SCRF models used for absorption assume that the ground state is in equilibrium with the solvent. The absorption process is assumed to be fast so that only the solvent electrons have time to rearrange in the new charge distribution created by the absorption. The solvent is assumed to be described as a continuum characterized by the dielectric constant, ε, and the refractive index, n. The slow response D', the polarization of the solvent due to nuclear motions, is defined through $g(\varepsilon) = g(D') + g(n^2)$, where g(x) represent the reaction of the medium to a charge distribution through modes "x", nuclear or electronic. The refractive index accounts for the fast response, the polarization of the solvent electrons. The interaction between the solvent and the dissolved molecule is assumed to be via dipole-dipole interaction only, although we

recognize the possible importance of higher moments. Acetonitrile is characterized here by ε=37.5 and n=1.3416.

We have four models for the SCRF calculations namely [12]:

1) In model A, solvent plus interaction energy the absorption energy is given by:

$$E^{A}_{abs} = \langle\Psi_f|H^A|\Psi_f\rangle - \langle\Psi_i|H^A|\Psi_i\rangle + 1/2\, g(\varepsilon)\langle\Psi_i|\mu|\Psi_i\rangle[\langle\Psi_f|\mu|\Psi_f\rangle - \langle\Psi_i|\mu|\Psi_i\rangle] + 1/2\, g(n^2)\langle\Psi_i|\mu|\Psi_i\rangle[\langle\Psi_i|\mu|\Psi_i\rangle - \langle\Psi_f|\mu|\Psi_f\rangle] \quad (1)$$

$$\mathbf{H}^A = \mathbf{H}_0 - g(\varepsilon)\langle\Psi_i|\mu|\Psi_i\rangle$$

2) In model B, solute plus solvent, the absorption energy is given by:

$$E^{B}_{abs} = \langle\Psi_f|H^B|\Psi_f\rangle - \langle\Psi_i|H^B|\Psi_i\rangle + 1/2\, g(n^2)\langle\Psi_i|\mu|\Psi_i\rangle [\langle\Psi_i|\mu|\Psi_i\rangle - \langle\Psi_f|\mu|\Psi_f\rangle] \quad (2)$$

$$\mathbf{H}^B = \mathbf{H}_0 - 1/2\, g(\varepsilon)\langle\Psi_i|\mu|\Psi_i\rangle$$

3) In model A1, solvent plus interaction energy in a mean field we assume that the absorption is fast but during the actual absorption the solvent electrons are in equilibrium with those of the solute. The absorption energy is then given by:

$$E^{A1}_{abs} = \langle\Psi_f|H^A|\Psi_f\rangle - \langle\Psi_i|H^A|\Psi_i\rangle + 1/2\, g(\varepsilon)\langle\Psi_i|\mu|\Psi_i\rangle[\langle\Psi_f|\mu|\Psi_f\rangle - \langle\Psi_i|\mu|\Psi_i\rangle] - 1/4\, g(n^2)[\langle\Psi_i|\mu|\Psi_i\rangle - \langle\Psi_f|\mu|\Psi_f\rangle]^2 \quad (3)$$

4) In model B1, solute plus solvent in a mean field the absorption energy is given by:

$$E^{B1}_{abs} = \langle\Psi_f|H^B|\Psi_f\rangle - \langle\Psi_i|H^B|\Psi_i\rangle - 1/4\, g(n^2)[\langle\Psi_i|\mu|\Psi_i\rangle - \langle\Psi_f|\mu|\Psi_f\rangle]^2 \quad (4)$$

In equation 1-4 $\langle\Psi_f|H|\Psi_f\rangle$, $\langle\Psi_i|H|\Psi_i\rangle$ represent the energy of the initial state and final state, respectively, after a CI calculation and $\langle\Psi_i|\mu|\Psi_i\rangle$, $\langle\Psi_f|\mu|\Psi_f\rangle$ are the state dipole moments of the initial and final state, respectively after the CI calculation. The g tensor is dependent on the shape and size of the cavity. In the case of a sphere the g tensor reduces to a scalar factor, $g(x) = 2(x-1)/((2x+1)a_0^3)$. First we investigate the spherical cavity with radius a_0. Mass density [12] yields a value for a_0 of 4.83 Å, which is a smaller cavity than the largest dimensions of the molecule. With this small

cavity the SCF problem converges to an unrealistic wave function independent of choice of SCRF model. The largest dimension of the molecule, calculated from the center of mass is about 6.6 Å. The outermost atoms are hydrogen and nitrogen. If we assume that the closest interaction distance between the solvent and the solute is given by the largest dimension of the molecule plus the van der Waals radii of the outermost atoms we calculate a solute cavity radius of 7.96 Å. Thus, we have compared the four different SCRF models with cavity radius ranging from 6.6 Å to 7.96 Å. The results are summarized in figure 4.

* fig. 4 *

All major peaks are blue shifted when the solute cavity size is decreased, and this is independent of the SCRF model as expected. The shift is proportional to the inverse of the third power of the cavity size and the state dipole moment differences, with different proportional constants depending on the model. Thus, the solvent stabilization is not the same for all states. The best agreement with the experimental spectrum is found for the smallest cavity corresponding to the largest dimension of the molecule, a_0=6.6 Å. The blue shift is due to the decrease of the dipole moment upon excitation, thus the ground state has the largest dipole moment and is stabilized more than the excited state. It appears that model B1 is the model that is least sensitive to the choice of cavity radius. Experience from calculations of emission spectra has also shown that the B1 model gives the most reasonable results [15], at least for volumes calculated from mass density. Calculations in reference 15 were performed with a SCRF method that allows the solvent electrons to fully relax in the reaction field and were found to yield results very similar to the first order perturbation treatment. For these reasons we use the B1 model with a_0=6.6 Å in all the following calculations of absorption spectra in solution.

The simulated absorption spectra in acetonitrile solution using different geometries are summarized in table 5. The energy of the first peak is calculated in good agreement with the experimental band for all geometries. Oscillator strengths are generally overestimated by a factor of two for the strongest bands by a CIS procedure, and this is also demonstrated here. The transition corresponds to a HOMO→LUMO transition and is $\pi\rightarrow\pi^*$. Using the crystallographic geometry the dipole moment decreases upon excitation and the transition corresponds to a charge transfer. When the calculated geometries are used in the spectral calculation the first peak is no longer predicted to be of charge transfer type. A shoulder is observed at 28100 cm^{-1}, and this is better reproduced using the calculated geometries that suggest a more "neutral" ground state. Although all transitions assigned to the observed shoulder are similar $\pi\rightarrow\pi^*$., that for the crystallographic structure and for the 4x4CI/PM3 model show considerable charge transfer (see the dipole moments). This shoulder is on a peak with maximum at

32000 cm^{-1}. All five calculations predict $\pi \rightarrow \pi^*$. transitions in this region, but the oscillator strengths of the transitions calculated between 22200 cm^{-1} and 35000 cm^{-1} is a sensitive function of geometry. The sum of the oscillator strengths, however, is relatively constant at 0.5. The calculations produce transitions between 37100 cm^{-1} and 48600 cm^{-1}, assigned to a second shoulder at about 45000 cm^{-1}, and they all yield several transitions from 49000 cm^{-1} and up, assigned to the broad band observed at about 50000 cm^{-1}. The best agreement between the observed absorption spectrum of α-P3CNQ in acetonitrile solution and the calculated absorption spectrum is obtained from the 4x4CI/PM3 optimized geometry or the SCRF optimized geometry (not shown). This spectrum is displayed in figure 5. The band shape has been obtained by superimposing a Lorentzian shaped functions centered on each calculate transition. The band width of each Lorentzian function was taken from the observed band width of the first strong peak, and the area is set equal to the calculated oscillator strength.

* Fig. 5*

As mentioned above, there is considerable charge transfer character calculated in the first transition when the experimental geometry, the 4x4CI/PM3 geometry and the SCRF/AM1 geometry are used. This gives us an excellent opportunity to determine if α-P3CNQ is best described as a zwitterion or not in solution. If the zwitterionic geometry is indeed the true geometry, the position of the charge transfer absorption peak at 16800 cm-1 will be highly solvent dependent whereas the "neutral" picture might suggest only a small dependence.

4. Summary.

We have obtained the geometry of α-P3CNQ using restricted Hartree-Fock theory with both semi-empirical and *ab initio* quantum chemistry, but none of the calculated geometries compares well with the x-ray geometry. Preliminary calculations that include electron correlation at the *ab initio* level did not improve these results. When we include the most important configurations needed to describe a biradical the resulting geometries agree much better with the observed geometry. The x-ray structure suggests a zwitterionic description of the molecule, whereas calculations that ignore condensed phase effects suggest a resonance mixture between neutral and zwitterionic form, see figure 2. The best agreement between the crystallographic geometry and calculated geometry is obtained with the SCRF/AM1 (a_0=6.6Å) calculation. We note that the geometry obtained at the HF/AM1 and HF/PM3 level compares very well with the geometry obtained at the HF/3-21G level although none of these compare well with experiment.

The best agreement between observed and calculated solution UV-visible spectrum is obtained using the 4x4CI/PM3 geometry. The 4x4CI/PM3 geometry is very similar to that predicted by the SCRF/AM1 with a slightly larger cavity (a_0=7.7Å). This indicates that the electrostatic effects are larger in the solid state then in acetonitrile solution. Furthermore, this suggests that the zwitterionic form is stabilized in polar solvents and in the solid state. The neutral picture is favored in non-polar solvents. The calculations of the solid state absorption spectrum show that the dimer interaction is very strong and that such interactions may be partially responsible for the stabilization of the zwitterionic geometry in the crystal. The first intense peak is red shifted by 1800 cm^{-1} when α-P3CNQ is dissolved in acetonitrile. We predicted a red shift by 600 cm^{-1} if the dimer spectrum is compare with the spectrum calculated in acetonitrile. This peak is predicted to have charge transfer character when using the crystallographic geometry. When using geometries obtained at the Hartree-Fock level the molecular orbitals are more delocalized thus, the first peak have less charge transfer character when these geometries are used. Futhermore, the closer the predicted geometry is to the crystallographic geometry the more charge transfer character is found for the first peak. We find a second peak at 22200 cm^{-1} that is not found in the experimental solution spectrum. When the HF optimized geometries are used this peak is moved up in energy and loose intensity. This second peak has a pronounced charge transfer character in all calculations. This peak might be identified as the small shoulder at 28100 cm^{-1} in the observed spectrum. If this indeed is the case our calculations indicate that the ground state of α-P3CNQ is best described as delocalized in solution and the zwitterionic geometry is stabilized in the crystal due to dimer interactions.

5. Acknowledgments.

This work was supported in part by grants from the Office of Naval Research and the Natural Science Foundation (CHE9312651). A. Broo is grateful for support from the Swedish Natural Science Research Council (NFR). Some of these calculations were supported by Florida State University through the allocation of super-computer resources.

6. References.

1. A. Broo, Chem. Phys. **169**, (1993), 135; Chem. Phys. **169**, (1993), 151.
2. A. Broo and M.C. Zerner, next article in this journal.
3. G.J. Ashwell, Thin Solid Films, **186**, (1990), 155.
4. R.M. Metzger, N.E. Heimer and G.J. Ashwell, Mol. Cryst. Liq. Cryst. **107**, (1984), 133.
5. S. Akhtar, J. Tanaka, R.M. Metzger and G.J. Ashwell, Mol. Cryst. Liq. Cryst. **139**, (1986), 353.
6. a) MOPAC 6.0 Program 455, Quantum Chemistry Exchange,
   b) AM1, M.J.S. Dewar, E.G. Zoebish, E.F. Healy, J.J.P. Stewart, J. Am. Chem. Soc. **107**, (1985), 3902.
   c) PM3, J.J.P. Stewart, J. Comp. Chem. **10**, (1989), 209.
   d) M.J.S. Dewar, J.A. Hashmall, C.G. Venier, J. Am. Chem. Soc. **90**, (1968), 1953.
   e) D.R. Armstrong, R. Fortune, P.G. Perkins and J.J.P. Stewart, J. Chem. Soc. Faraday II, **68**, (1972), 1839.
   f) M.J.S. Dewar, D.A. Liotard, J. Mol. Struct. (Theochem), **206**, (1990), 123.
7. a) W.J. Hehre, R.F. Stewart, J.A. Pople, J. Chem. Phys. **51**, (1969), 2657.
   b) J.S. Binkley, J.A. Pople, W.J. Hehre, J. Am. Chem. Soc. **102**, (1980), 939.
8. P.C. Hariharan, J.A.Pople, Theoret. Chim. Acta **28**, (1973), 21
9. GAMESS, M.W.Schmidt, K.K. Baldridge, J.A. Boatz, T.S. Elbert, M.S. Gordon, J.H. Jensen, S. Koseki, N. Matsunaga, K.A. Nguyen, S. Su, T.L. Windus, M. Dupuis, J.A. Montgomery Jr. J. Comp. Chem. **14**, (1993), 1347.
10. Gaussian 92, Revision B, M.J. Frisch, G.W. Trucks, M. Head-Gordon, P.M. W. Gill, M.W. Wong, J.B. Foresman, B.G. Johnson, H.B. Schlegel, M.A. Robb, E.S. Replogle, R. Gomperts, J.L. Andres, K. Raghavachari, J.S. Binkley, C. Gonzalez, R.L. Martin, D.J. Fox, D.J. Defrees, J. Baker, J.J.P. Stewart, and J.A. Pople, Gaussian, Inc., Pittsburgh PA, 1992.
11. ZINDO M.C. Zerner, Quantum Theory Project, University of Florida, Gainesville, Fl 32 611; see also J.E. Ridley and M.C. Zerner, Theoret Chim. Acta **32**, (1973), 111.
12. M.M. Karelson and M.C. Zerner, Int. J. Quant. Chem. Symp. **20**, (1986), 521; M.M. Karelson and M.C. Zerner, J. Phys. Chem. **96**, (1992), 8991.
13. P.J. Hay, J.C. Thibeault and R. Hoffmann, J. Am. Chem. Soc. **97**, (1975), 4884.
14. G.J. Ashwell, J.R. Sambles, A.S. Martin, M.G. Parker, M. Szablewski, J. Chem. Soc. Chem. Commun. **19**, (1990), 1374.
15. A. Broo and M.C. Zerner, Chem. Phys. Letters **227**, (1994), 551.

7. Figure and table legends

Figure 1. The geometry of Z-β–(1-methyl-2-pyridinium)-α-cyano-4-styryldicyanomethanide (α-P3CNQ) also shown is the labeling of the atoms.

Figure 2. Resonance structures of α-P3CNQ. a) The "neutral "resonance structure. b-d) the three different zwitterionic or biradical resonance structures.

Figure 3. The HF/AM1 calculated vibration spectra of α-P3CNQ using the optimized geometry. All frequencies are scaled with a factor of 0.85.

Figure 4. A comparison of how the calculated absorption energies, using the crystallographic geometry, of the three first most intense peaks of α-P3CNQ vary as a function of the solvation cavity radius a_0. a) SCRF method A, b) SCRF method A1, c) SCRF method B and d) SCRF method B1.

Figure 5. The predicted absorption spectrum of α-P3CNQ using acetonitrile as solvent. The 4x4CI/PM3 geometry is used in the INDO/S-SCRF calculation. The band shape is obtained by superimpose Lorentzian functions centered at each calculated peak. The width of each Lorentzian function was obtained from the observed band width of the major band at 16800 cm^{-1}.

Table 1. A summary of the predicted geometries of α-P3CNQ at different level of restricted Hartree-Fock theory compared with the crystallographic geometry. The labeling of the atoms is shown in figure 1. Bold face numbers indicate the important bridge bonds. a) Observed geometry is from reference 4.

Table 2. A summary of the predicted geometries of α-P3CNQ using a semi-empirical 4x4CI approach, a ^3A state using a ROHF/STO-3G approach, a second-order Møller-Plesset perturbation theory with the STO-3G basis set and two SCRF calculations with the AM1 Hamiltonian. The labeling of the atoms is shown in figure 1. Bold face numbers indicate the important bridge bonds. a) Observed geometry is from reference 4.

Table 3a. A summary of the Mulliken charges and dipole moments of α-P3CNQ obtained at the RHF optimized geometries and the crystallographic geometry. The labeling of the atoms is shown in figure 1.

Table 3b. Summary of the Mulliken charges and dipole moments of α-P3CNQ at the 4x4CI/AM1 and 4x4CI/PM3, ^{3}A *ab initio* ROHF/STO-3G and MP2/STO-3G optimized geometries. a) 4x4CI/AM1 and 4x4CI/PM3 results using the crystallographic geometry. b) The ^{3}A result. The labeling of the atoms is shown in figure 1.

Table 4. Calculated absorption spectrum of a monomer and a dimer of α-P3CNQ compared with the experimental solid state spectrum from reference 5. The experimental oscillator strength for the high energy band was not calculated because of the presence of many unresolved overlapping bands.

Table 5. Calculated absorption spectra of α-P3CNQ in acetonitrile solution compared with the observed spectrum from reference 5, using SCRF model B1, see text.

Table 1

	HF/AM1	HF/PM3	HF/STO-3G	HF/3-21G	HF/6-31G*	Observed[a]
Bonds						
C1-C2	**1.435**	**1.434**	**1.470**	**1.436**	**1.442**	**1.355**
C2-C3	**1.374**	**1.377**	**1.360**	**1.370**	**1.369**	**1.467**
C3-C4	1.450	1.448	1.474	1.450	1.452	1.404
C2-C5	1.430	1.432	1.469	1.438	1.453	1.442
C5-N6	1.165	1.161	1.157	1.141	1.136	1.135
C4-C7	1.351	1.348	1.328	1.337	1.337	1.374
C7-C8	1.451	1.450	1.475	1.451	1.452	1.398
C3-C9	1.450	1.449	1.474	1.449	1.452	1.396
C8-C10	1.451	1.450	1.476	1.452	1.454	1.411
C9-C10	1.351	1.347	1.328	1.336	1.337	1.366
C8-C11	1.369	1.367	1.356	1.362	1.365	1.440
C11-C12	1.420	1.422	1.455	1.420	1.435	1.412
C12-N13	1.164	1.161	1.158	1.142	1.138	1.148
C11-C14	1.420	1.422	1.455	1.420	1.435	1.408
C14-N15	1.164	1.161	1.158	1.142	1.138	1.143
C1-C16	**1.380**	**1.375**	**1.354**	**1.375**	**1.377**	**1.454**
C16-C17	1.456	1.444	1.477	1.443	1.446	1.381
C17-C18	1.359	1.356	1.331	1.343	1.343	1.367
C18-C19	1.428	1.427	1.453	1.427	1.429	1.379
C16-N20	1.406	1.418	1.422	1.384	1.381	1.374
C19-C21	1.370	1.360	1.330	1.338	1.338	1.349
N20-C22	1.440	1.476	1.475	1.474	1.457	1.470
Mean	0.039	0.038	0.055	0.035	0.039	
difference	(0.026)	(0.026)	(0.032)	(0.029)	(0.029)	
Torsion angles						
α	10.05	9.21	6.06	11.11	10.45	33.49
β	7.01	2.75	6.48	10.63	10.26	4.71
γ	36.99	25.69	31.23	27.20	28.21	3.32

Table 2.

	4x4CI/ AM1	4x4CI/ PM3	^{3}A ROHF/ STO-3G	MP2/ STO-3G	SCRF AM1 a_0=7.7Å	SCRF AM1 a_0=6.6Å	Observed[a]
Bonds							
C1-C2	**1.398**	**1.396**	**1.361**	**1.457**	**1.385**	**1.357**	**1.355**
C2-C3	**1.423**	**1.425**	**1.501**	**1.427**	**1.414**	**1.445**	**1.467**
C3-C4	1.423	1.424	1.400	1.477	1.433	1.413	1.404
C2-C5	1.424	1.426	1.452	1.484	1.435	1.435	1.442
C5-N6	1.165	1.162	1.158	1.232	1.165	1.164	1.135
C4-C7	1.371	1.366	1.380	1.376	1.364	1.378	1.374
C7-C8	1.430	1.427	1.398	1.479	1.434	1.421	1.398
C3-C9	1.422	1.421	1.399	1.476	1.424	1.411	1.396
C8-C10	1.428	1.425	1.396	1.479	1.433	1.425	1.411
C9-C10	1.372	1.368	1.381	1.377	1.369	1.381	1.366
C8-C11	1.395	1.396	1.486	1.398	1.390	1.413	1.440
C11-C12	1.416	1.418	1.450	1.476	1.412	1.403	1.412
C12-N13	1.165	1.162	1.159	1.231	1.167	1.169	1.148
C11-C14	1.416	1.418	1.450	1.476	1.412	1.403	1.408
C14-N15	1.165	1.162	1.159	1.231	1.167	1.170	1.143
C1-C16	**1.404**	**1.399**	**1.428**	**1.405**	**1.429**	**1.464**	**1.454**
C16-C17	1.449	1.437	1.450	1.483	1.438	1.410	1.381
C17-C18	1.362	1.359	1.338	1.376	1.376	1.395	1.367
C18-C19	1.427	1.423	1.453	1.460	1.412	1.399	1.379
C16-N20	1.398	1.415	1.426	1.447	1.384	1.382	1.374
C19-C21	1.370	1.360	1.331	1.375	1.384	1.399	1.349
N20-C22	1.385	1.403	1.410	1.420	1.451	1.455	1.470
Mean deviation	0.026 (0.017)	0.026 (0.017)	0.026 (0.022)	0.060 (0.030)	0.025 (0.017)	0.018 (0.011)	
Torsion angles							
α	21.18	18.40	10.56	0.05	36.96	39.93	33.49
β	16.10	4.44	28.05	0.06	14.48	8.62	4.71
γ	17.26	8.58	4.37	0.10	8.23	3.95	3.32

Table 3a

	HF/AM1	HF/AM1[a]	HF/PM3	HF/STO-3G	HF/3-21G	HF/6-31G*
E(a.u.)	-120.9884	-120.7088	-108.7959	-895.05791	-901.25758	-906.32025
μ(D)	10.84	21.51	11.43	10.36	15.65	15.41
C1	-0.31	-0.32	-0.35	-0.14	-0.31	-0.39
C2	0.14	0.17	0.20	0.04	0.05	0.08
C3	-0.09	-0.17	-0.13	0.00	-0.11	-0.05
C4	-0.07	-0.04	-0.03	-0.04	-0.18	-0.17
C5	-0.11	-0.12	-0.11	0.06	0.31	0.26
N6	-0.03	-0.02	-0.06	-0.19	-0.51	-0.46
C7	-0.16	-0.16	-0.15	-0.07	-0.23	-0.24
C8	0.09	0.11	0.08	0.07	-0.01	0.11
C9	-0.06	-0.05	-0.04	-0.04	-0.17	-0.16
C10	-0.16	-0.18	-0.15	-0.07	-0.23	-0.23
C11	-0.01	-0.14	0.06	-0.02	0.00	-0.09
C12	-0.09	-0.05	-0.09	0.07	0.33	0.30
N13	-0.04	-0.09	-0.06	-0.19	-0.52	-0.47
C14	-0.09	-0.05	-0.09	0.07	0.33	0.30
N15	-0.04	-0.09	-0.06	-0.19	-0.52	-0.47
C16	0.15	0.15	0.03	0.15	0.50	0.49
C17	-0.19	-0.15	-0.16	-0.08	-0.30	-0.28
C18	-0.05	-0.01	-0.03	-0.03	-0.15	-0.13
C19	-0.23	-0.17	-0.16	-0.10	-0.38	-0.31
N20	-0.18	-0.11	0.24	-0.25	-1.03	-0.74
C21	0.00	0.02	-0.14	0.07	0.26	0.15
C22	-0.09	-0.03	-0.12	-0.07	-0.35	-0.31
H23	0.16	0.15	0.13	0.09	0.28	0.24
H24	0.14	0.14	0.13	0.06	0.24	0.21
H25	0.14	0.12	0.11	0.09	0.28	0.26
H26	0.15	0.13	0.12	0.08	0.28	0.25
H27	0.14	0.11	0.11	0.08	0.26	0.23
H28	0.15	0.13	0.12	0.08	0.28	0.25
H29	0.16	0.15	0.13	0.08	0.29	0.25
H30	0.15	0.15	0.11	0.08	0.28	0.24
H31	0.16	0.14	0.13	0.08	0.26	0.23

H32	0.09	0.09	0.06	0.08	0.24	0.20
H33	0.10	0.11	0.07	0.08	0.23	0.20
H34	0.10	0.09	0.07	0.09	0.26	0.21
			Sum of group charges			
Donor	0.33	0.57	0.39	0.25	0.39	0.48
bridge	-0.19	-0.14	-0.19	-0.17	-0.18	-0.30
Acceptor	-0.14	-0.43	-0.20	-0.08	-0.21	-0.18

Table 3b

	AM1	AM1[a]	PM3	PM3[a]	ROHF	MP2
E(a.u.)	-120.9896	-120.7242	-108.7984	-108.5722	-895.05616	-896.48194
μ(D)	12.53	9.52	12.53	9.46	8.09	14.13
C1	-0.16	-0.07	-0.13	-0.05	-0.05	-0.13
C2	-0.01	-0.06	0.02	0.03	-0.03	0.05
C3	0.00	0.03	0.01	0.03	0.03	-0.02
C4	-0.12	-0.12	-0.11	-0.10	-0.07	-0.04
C5	-0.09	-0.09	-0.08	-0.09	0.06	0.05
N6	-0.06	-0.06	-0.09	-0.08	-0.22	-0.17
C7	-0.11	-0.07	-0.08	-0.03	-0.05	-0.07
C8	0.01	-0.02	-0.01	-0.04	0.00	0.06
C9	-0.13	-0.13	-0.12	-0.11	-0.07	-0.04
C10	-0.11	-0.09	-0.08	-0.06	-0.05	-0.07
C11	0.00	0.04	0.09	0.13	0.06	-0.03
C12	-0.09	-0.09	-0.10	-0.11	0.07	0.05
N13	-0.04	-0.08	-0.06	-0.03	-0.17	-0.19
C14	-0.09	-0.09	-0.10	-0.11	0.07	0.05
N15	-0.04	-0.02	-0.05	-0.04	-0.17	-0.19
C16	0.03	-0.05	-0.14	-0.25	0.09	0.15
C17	-0.11	-0.05	-0.06	0.01	-0.07	-0.08
C18	-0.10	-0.13	-0.08	-0.12	-0.05	-0.02
C19	-0.19	-0.15	-0.13	-0.09	-0.09	-0.09
N20	-0.14	-0.14	0.31	0.35	-0.25	-0.24
C21	-0.02	0.00	-0.17	-0.17	0.00	0.08

C22	-0.09	-0.03	-0.13	-0.07	-0.07	-0.06
H23	0.16	0.13	0.13	0.10	0.08	0.09
H24	0.13	0.12	0.11	0.10	0.07	0.06
H25	0.15	0.14	0.12	0.11	0.07	0.08
H26	0.15	0.12	0.12	0.09	0.08	0.08
H27	0.13	0.12	0.11	0.10	0.08	0.07
H28	0.15	0.13	0.11	0.10	0.07	0.07
H29	0.17	0.14	0.13	0.10	0.08	0.09
H30	0.15	0.14	0.12	0.11	0.09	0.09
H31	0.16	0.13	0.12	0.09	0.07	0.08
H32	0.10	0.09	0.07	0.05	0.08	0.09
H33	0.10	0.09	0.07	0.05	0.09	0.08
H34	0.11	0.07	0.07	0.04	0.08	0.09
			Sum of group charges			
Donor	0.30	0.23	0.32	0.15	0.22	0.33
bridge	-0.15	-0.16	-0.17	-0.09	-0.17	-0.14
Acceptor	-0.15	-0.07	-0.15	-0.06	-0.05	-0.19

Table 4

Calculated, monomer		Calculated, dimer		Experimental, reference 5		
E(kK)	*f*osc	E(kK)	*f*osc	E(kK)	*f*osc	Type
		13.4	0.00	11.8		⊥ b(100)
				12.4		∥ b(001)
				12.4		∥ b(100)
14.1	1.63	15.1	2.60	18.6	2.23	⊥ b(001)
		17.0	0.0			
19.5	0.34	17.0	0.0			
		21.0	0.0			
25.9	0.05	21.2	0.60	21.8	0.16	⊥ b(100)
		26.1	0.0			
28.3	0.04	26.1	0.0			
		27.3	0.0			
28.9	0.05	27.5	0.27			
		28.7	0.06			
31.2	0.0	28.7	0.0			
		29.1	0.14			
32.4	0.12	29.3	0.0	32.0	?	⊥ b(001)
		32.2	0.03			
35.3	0.0	32.2	0.0			
		33.0	0.24			
37.5	0.02	33.0	0.0			
		34.1	0.0			

Table 5

Crystallographic geometry. Ground state dipole moment 34.7 Debye.

Energy (kK)	14.5	22.2	28.7	29.7	33.4	33.8	41.1	47.7	51.2
*f*osc	1.14	0.20	0.19	0.04	0.04	0.08	0.07	0.07	0.14
μ (Debye)	13.6	8.7	15.4	18.1	19.9	20.8	21.6	19.6	26.2

HF/PM3 geometry. Ground state dipole moment 17.0 Debye.

Energy (kK)	17.5	27.5	29.9	32.5	33.3	37.1	50.5	52.0
*f*osc	1.75	0.04	0.47	0.03	0.02	0.10	0.09	0.19
μ (Debye)	22.3	6.9	15.8	20.3	17.4	12.2	8.9	18.3

HF/6-31G* geometry. Ground state dipole moment 17.3 Debye.

Energy (kK)	17.4	27.5	30.3	32.3	33.1	37.1	50.4	51.5
*f*osc	1.74	0.03	0.42	0.03	0.03	0.09	0.09	0.13
μ (Debye)	22.5	7.4	16.5	21.1	17.0	12.6	13.8	13.1

4x4CI/PM3 geometry. Ground state dipole moment 24.7 Debye.

Energy (kK)	16.2	25.7	29.5	30.0	32.0	34.9	48.6	51.8	54.2
*f*osc	1.97	0.03	0.13	0.04	0.04	0.07	0.13	0.22	0.23
μ (Debye)	18.9	6.5	16.9	24.4	13.1	18.9	20.4	21.1	16.1

SCRF/AM1 a_0=6.6Å geometry. Ground state dipole moment 35.7 Debye.

Energy (kK)	14.3	21.5	27.3	29.0	32.8	39.4	46.1	50.3	50.8
*f*osc	1.03	0.25	0.09	0.11	0.10	0.04	0.10	0.12	0.09
μ (Debye)	14.2	10.6	13.8	21.5	25.8	24.4	26.0	30.7	14.4

Observed absorption spectrum *f*osc	16.8 Sharp peak 0.49	28.1 Small shoul-der	32.0 Broad band			35.0 Small shoul-der	45.0 Shoul-der	50.0- Broad band	

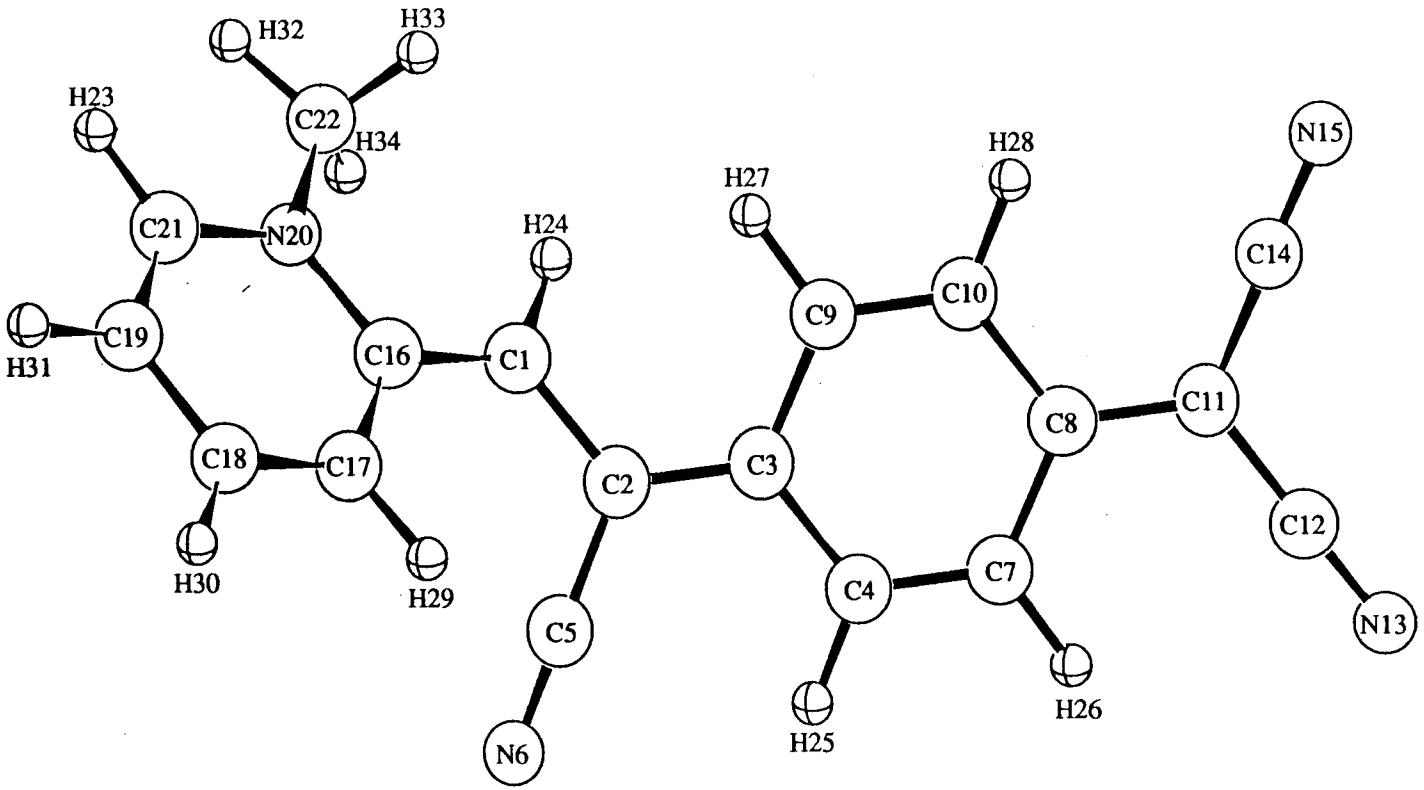
H32
H33
H23
C22
H34
C21
N20
H24
H27
H28
N15
C14
C19
C16
C1
C9
C10
H31
C11
C8
C18
C17
C2
C3
C12
H30
H29
C4
C7
C5
N13
H26
H25
N6

Fig. 1

a)

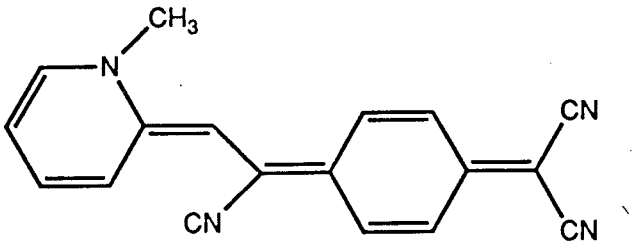

b)

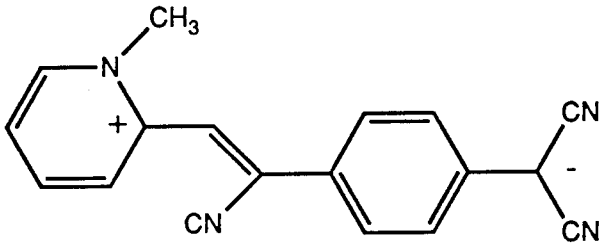

c)

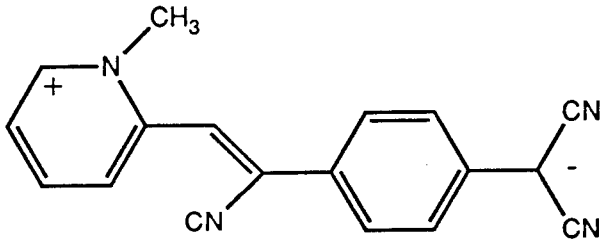

d)

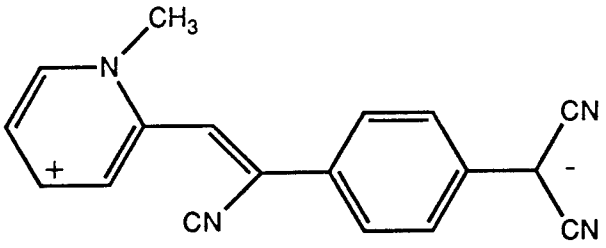

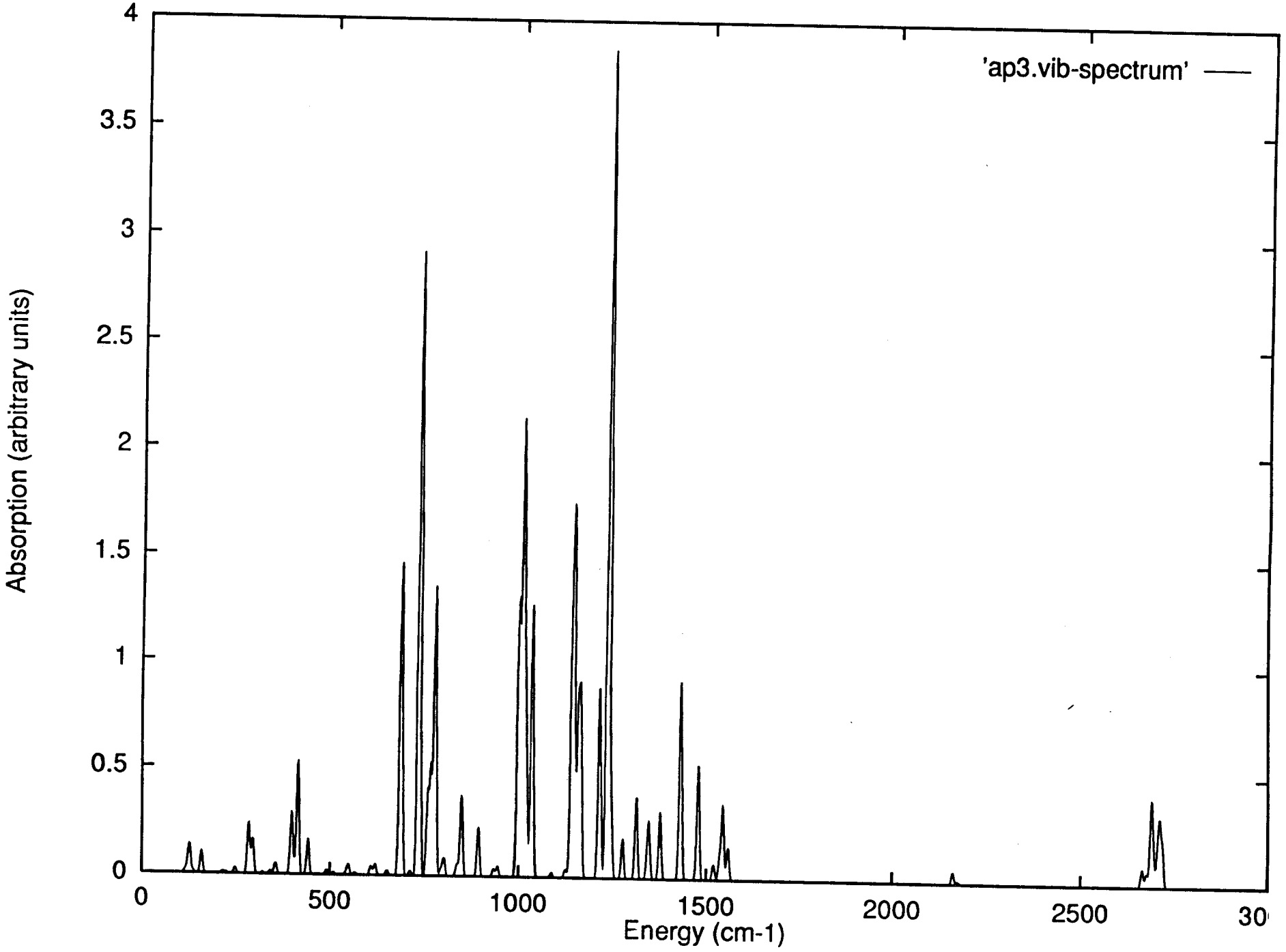
'ap3.vib-spectrum'
Absorption (arbitrary units)
Energy (cm-1)
0
0.5
1
1.5
2
2.5
3
3.5
4
0
500
1000
1500
2000
2500
30

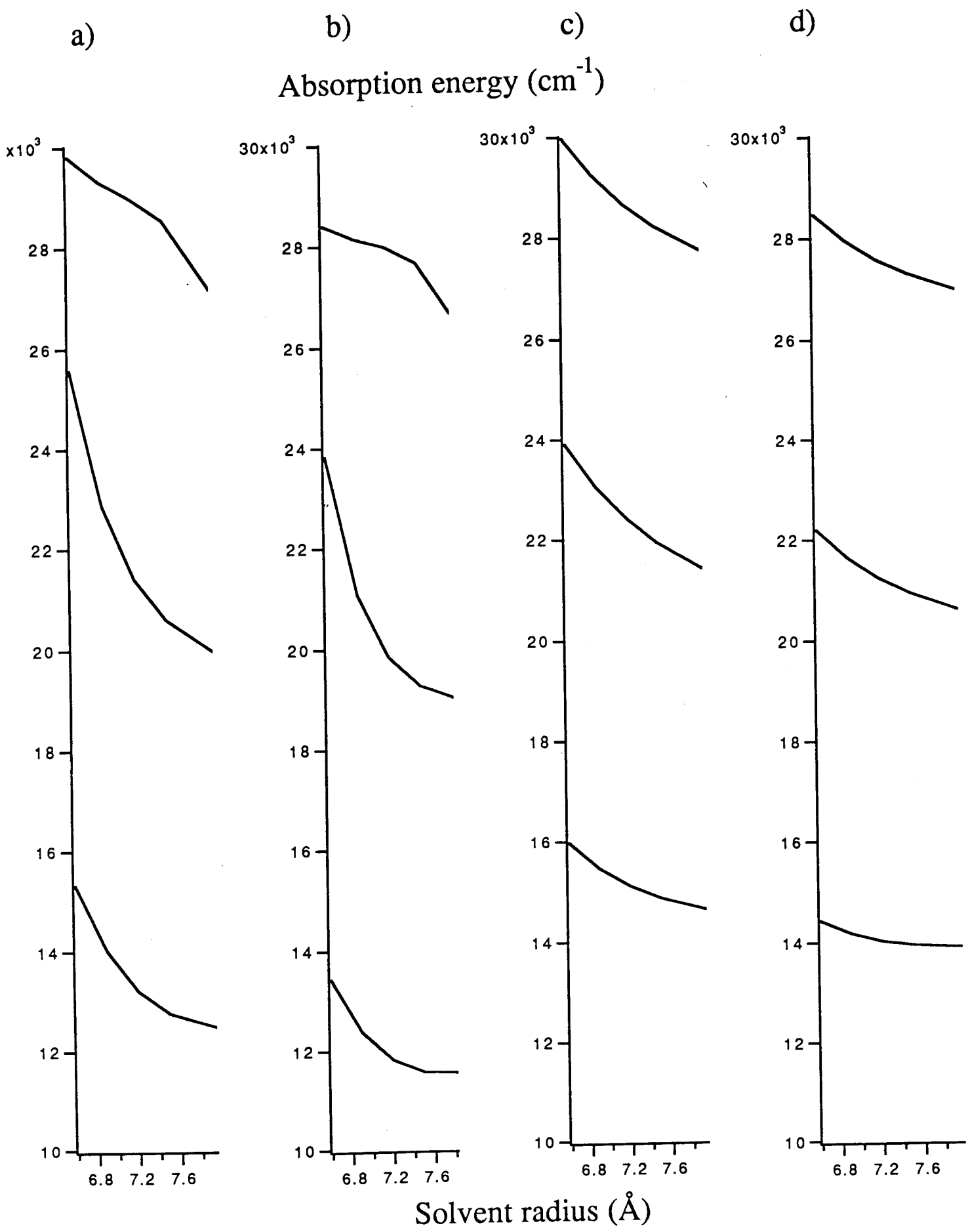
a)
b)
c)
d)
Absorption energy (cm-1)
x10^3
30x10^3
30x10^3
30x10^3
28
26
24
22
20
18
16
14
12
10
6.8
7.2
7.6
Solvent radius (Å)

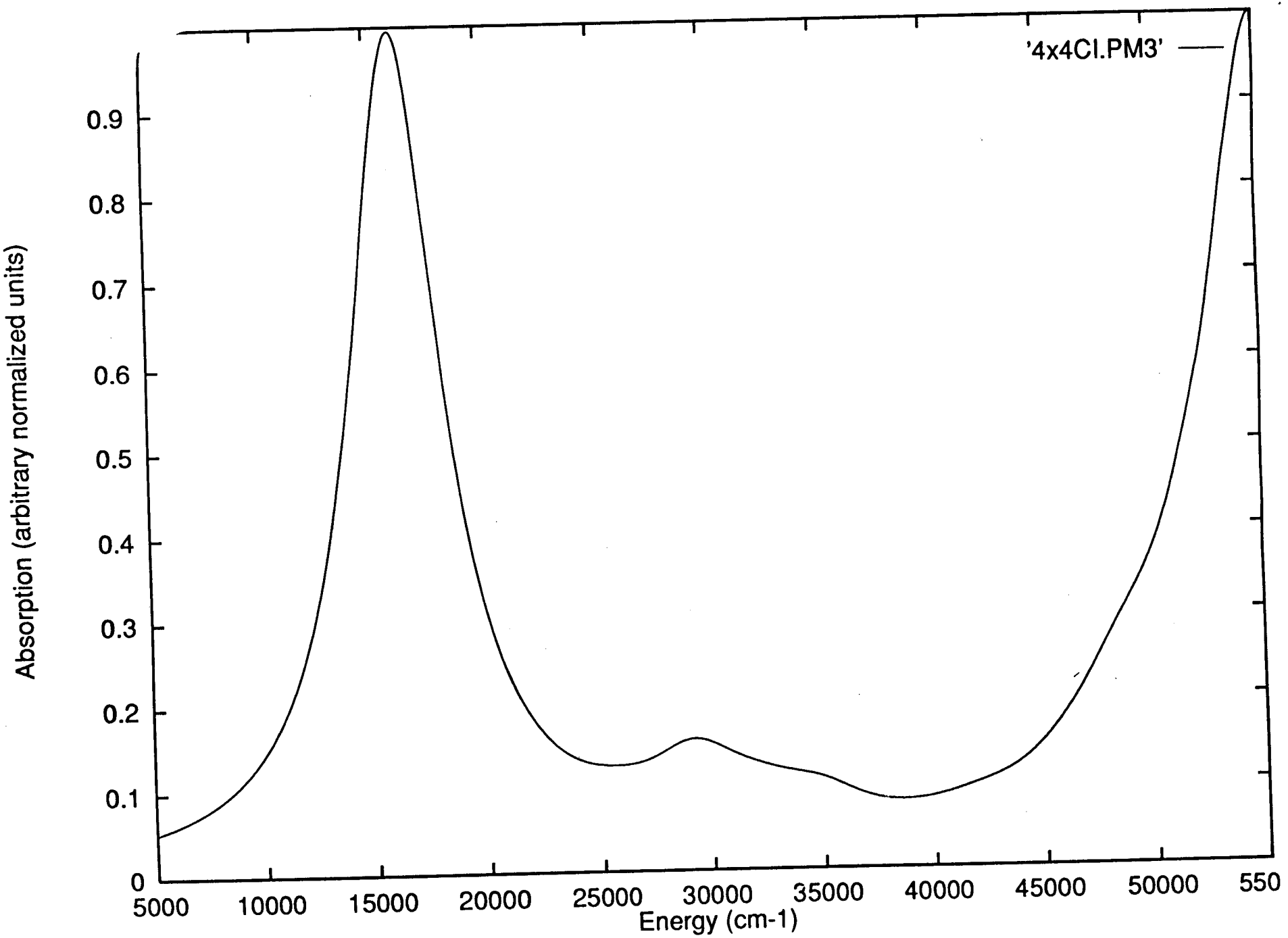
'4x4Cl.PM3'
Absorption (arbitrary normalized units)
0
0.1
0.2
0.3
0.4
0.5
0.6
0.7
0.8
0.9
5000
10000
15000
20000
25000
30000
35000
40000
45000
50000
550
Energy (cm-1)